AGU PUBLICATIONS

Geophysical Research Letters

RESEARCH LETTER
10.1002/2016GL069692

Special Section:
First results from NASA's Magnetospheric Multiscale (MMS) Mission

Stable reconnection at the dusk flank magnetopause

R. G. Gomez[1], S. K. Vines[1,2], S. A. Fuselier[1,2], P. A. Cassak[3], R. J. Strangeway[4], S. M. Petrinec[5], J. L. Burch[1], K. J. Trattner[6], C. T. Russell[4], R. B. Torbert[7], C. Pollock[8], D. T. Young[1], W. S. Lewis[1], and J. Mukherjee[1]

[1]Southwest Research Institute, San Antonio, Texas, USA, [2]University of Texas at San Antonio, San Antonio, Texas, USA, [3]Department of Physics and Astronomy, West Virginia University, Morgantown, West Virginia, USA, [4]Institute of Geophysics and Planetary Physics, University of California, Los Angeles, California, USA, [5]Lockheed Martin ATC, Palo Alto, California, USA, [6]Laboratory for Atmospheric and Space Physics, University of Colorado Boulder, Boulder, Colorado, USA, [7]The Johns Hopkins University Applied Physics Laboratory, Laurel, Maryland, USA, [8]NASA/GSFC, Greenbelt, Maryland, USA

Abstract The dusk flank magnetopause was surveyed with instruments on board the Magnetospheric Multiscale (MMS) spacecraft on 28 August 2015 between 13:55 UT and 14:15 UT during a period of persistent southward interplanetary magnetic field (IMF) with varying dawn-dusk component. Plasma measurements (500 eV electrons, $>$ 2 keV ions) revealed the existence of at least one active reconnection region that persisted throughout the interval. The reconnection region convected equatorward despite the poleward and tailward magnetosheath flow, which ranged from slightly sub-Alfvénic to slightly super-Alfvénic throughout the interval. These results suggest that magnetic reconnection moved in response to changes in the IMF clock angle rather than the magnetosheath flow, which is corroborated using predictions of the maximum magnetic shear model.

Key Points:
- Asymmetric magnetic reconnection with a flow shear is a stable process in the dusk flank magnetopause
- Reconnection site motion is coupled to changes in the IMF clock angle
- The reconnection line can shift equatorward against magnetosheath bulk flow in response to upstream IMF changes

Supporting Information:
- Movie S1
- Supporting information S1

Correspondence to:
R. G. Gomez,
rgomez@swri.edu

Citation:
Gomez, R. G., et al. (2016), Stable reconnection at the dusk flank magnetopause, *Geophys. Res. Lett.*, *43*, 9374–9382, doi:10.1002/2016GL069692.

Received 31 MAY 2016
Accepted 2 AUG 2016
Accepted article online 8 AUG 2016
Published online 17 SEP 2016

1. Introduction

Magnetic reconnection is the dominant process for the transfer of mass, energy, and momentum from the solar wind into the Earth's magnetosphere. For a southward oriented interplanetary magnetic field (IMF) on the dayside magnetopause, a single reconnection line forms across the magnetosphere, spanning from the dusk flank to the dawn flank [*Moore et al.*, 2002; *Phan et al.*, 2006; *Trattner et al.*, 2007a, 2007b; *Vines et al.*, 2015].

The presence of the reconnection line is identified by accelerated ion and electron flows. *Gosling et al.* [1990] observed accelerated plasma flows in the lower latitude boundary layer (LLBL) of the magnetosphere. In a later study, *Phan et al.* [2006] reported Wind, ACE, and Cluster measurements of accelerated particle flows resulting from a reconnection line at least 390 R_E in length in the solar wind. Their observations revealed that reconnection can operate in a quasi-steady state manner and forms long reconnection lines even when not driven by an external flow.

Generally, plasma instruments are able to observe and measure the direction and energy of particle flows from reconnection events. Examples of these measurements are found in *Fuselier et al.* [1997, 2011]. In *Fuselier et al.* [1997], Active Magnetospheric Particle Tracer Explorers-Charge Composition Explorer measurements of fast electron flows (above 50 eV) were shown to be an indicator of transitions between the magnetosheath and open field lines in the magnetosheath boundary layer (MSBL). Their correlation to the topology of the local magnetic field was also shown to be an indicator of ongoing magnetic reconnection. It is important to note here that while the direction and energy of the particle flows are measurable by such instruments, the distance from the instrument to the reconnection site must be determined using other methods.

To determine the most probable location of the reconnection line, *Trattner et al.* [2007a, 2007b] developed the maximum magnetic shear model. This model uses the upstream IMF (convected to the magnetopause from ACE and Wind observations) to determine the magnetic shear angle between the draped magnetosheath magnetic field (using the Cooling draping model) and the magnetospheric field (using the Tsyganenko T96 magnetic field model). It then places the reconnection line according to the empirical results from POLAR-Toroidal Imaging Mass-Angle Spectrograph observations. The reconnection line observed for the southward IMF generally spans the entire dayside magnetopause. The locations at the flanks and subsolar point depend on the dipole tilt angle and IMF B_y directions.

While many investigations have focused on the dayside magnetopause near the subsolar region for southward IMF, several studies have shown evidence of reconnection on the flanks [e.g., *Gosling et al.*, 1986;

Phan et al., 2000; 2006]. *Gosling et al.* [1986] reported ISEE 1 and ISEE 2 observations of accelerated particle flows at the near-tail dusk flank and attributed these flows to nearly antiparallel reconnection occurring tailward of the terminator. Bidirectional plasma jets have also been detected at the dawn flank magnetopause in conjunction with observations of accelerated flows at the subsolar point [*Phan et al*., 2000; 2006]. The presence of bidirectional jets provides clear evidence of a stable reconnection line that can extend at least 10 R_E across the magnetopause. Antiparallel reconnection on both flanks extending to the terminator is also predicted by the maximum shear magnetic model.

The spatial expanse and temporal persistence of the reconnection region are subjects in several studies [e.g., *Phan et al*., 2000; 2006; *Frey et al*., 2003; *Trattner et al*., 2007a; 2007b; *Trenchi et al*., 2008, *Hasegawa et al*., 2016]. The overall results of these studies show that the temporal duration of the reconnection region is long (tens of minutes to hours) for steady southward IMF, and the spatial expanse is large (tens of R_E for the dayside magnetopause and up to hundreds in the solar wind).

Previous observations [e.g., *Petrinec et al*., 2003; *Wilder et al*., 2014] and theory [e.g., *Cowley and Owen*, 1989; *Doss et al*., 2015] point to the existence of open magnetic flux convecting in the presence of a large magnetosheath flow. The observations of *Wilder et al*. [2014] indicate that a reconnection X line propagates tailward at velocities comparable to that of the magnetosheath bulk flow. Theoretical results of *Doss et al*. [2015], supported by simulations, predict that open flux from an asymmetric reconnection X line convects for a large range of flow shears, not limited to super-Alfvénic velocities. These results are to be contrasted with observations by *Fuselier et al.* [2000] and *Petrinec et al.* [2003] which demonstrated stationary reconnection sites (presumably not for open flux) for sub-Alfvénic velocities but suggest tailward convecting reconnection sites for super-Alfvénic speeds. These observations have largely been made during intervals of northward IMF. However, the motion of reconnection sites equatorward of the cusps during southward IMF has not been well investigated.

The purpose of this paper is to present new observations by the Magnetospheric Multiscale (MMS) mission [*Burch et. al*, 2015] at the dusk terminator of a stable reconnection region. While the reconnection region encountered was stable in time, the motion of the reconnection site during this interval was at times equatorward, so appears to be dictated by changes in the IMF clock angle, despite the presence of a large southward magnetosheath flow.

2. Observations

Observations of the duskside magnetopause were made by instruments aboard the MMS spacecraft on 28 August 2015. All of the observations presented here are from MMS-4. This is because, at this time, MMS-4 had the only fully commissioned and operational instrument suite. Moments of the ion distributions (particularly, the flow velocity in the magnetosheath), plasma composition, and the identification of the boundary layers and magnetopause current layer are from the Hot Plasma Composition Analyzer (HPCA) instrument [*Young et al*., 2014]. The distributions of higher-energy protons (tens of keV) from HPCA are also used to determine the relative direction to the reconnection site. Magnetic field measurements from the Digital Fluxgate Magnetometer (DFG) [*Russell et al*., 2014] are used to identify the boundary layers in conjunction with HPCA. These measurements are also used to determine the pitch angle of particles streaming parallel or antiparallel with respect to the local magnetic field. The Electron Drift Investigation (EDI) [*Torbert et al.,* 2016] operating in the ambient mode (corresponding to an electron energy of 500 eV) is used to measure electron counts to determine the streaming direction of electrons from the reconnection site, i.e., to locate the direction of the reconnection site relative to MMS. Omnidirectional electron flux from the Fast Plasma Investigation Dual Electron Spectrometer (FPI-DES) [*Pollock et al*., 2016] is also used to identify regions during this encounter with the magnetopause. Upstream solar wind conditions and IMF clock angle, convected to the magnetopause, are from the ACE and Wind spacecraft.

During the magnetopause crossings on 28 August 2015, MMS was at the dusk flank magnetopause, just south of the equator near the dusk terminator. MMS encountered the magnetopause several times over the interval from 12:00 UT to 15:30 UT. Signatures of reconnection, such as plasma jets, were observed during the magnetopause crossings throughout this several hour period (not shown). The IMF was oriented southward during this time, with a large negative B_y (pointing dawnward). This configuration of the upstream IMF allowed for reconnection along the dusk flank over this long interval (see supporting information Movie S1).

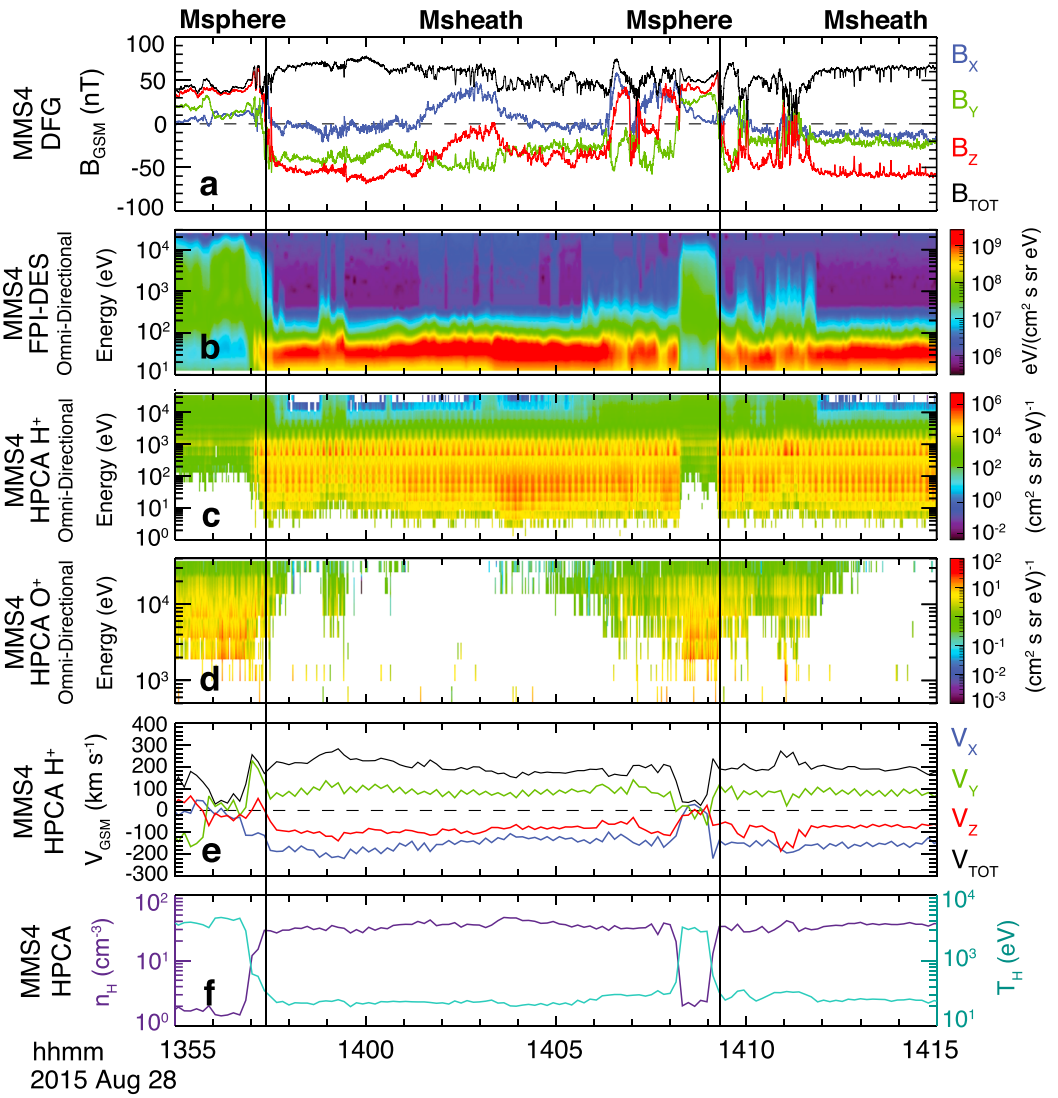

Figure 1. Encounter with the magnetopause and boundary layers on the Southern Hemisphere dusk flank by MMS4 on 28 August 2015 from 13:55 to 14:15 UT. (a) Magnetic field in GSM coordinates from DFG. (b) Omnidirectional electron energy flux from FPI-DES. (c) Omnidirectional H^+ flux from HPCA. (d) Omnidirectional O^+ flux from HPCA. (e) H^+ velocity components (km/s, in GSM) from HPCA. (f) H^+ density (deep purple, in cm^{-3}) and scalar temperature (mint green, in eV). The leftmost vertical black line marks the initial magnetopause crossing at 13:57:23 UT. The rightmost vertical black line marks a second magnetopause crossing by MMS4 at 14:09:17 UT after a brief reentry into the magnetosphere starting around 14:06 UT.

Figure 1 displays the measurements made by MMS-4 during the magnetopause crossing from 13:55 UT to 14:15 UT. The average position of MMS4 (in GSM) were $(X, Y, Z) = (2.4, 9.8, -5.2)\ R_E$ at the time of the observations. The spacecraft begins in the magnetosphere at 13:55 UT, as indicated by the DFG measurements in Figure 1a, which show a positive z component of the magnetic field ($+B_z$). The temperatures (Figure 1f, mint green) and proton densities (Figure 1f, deep purple) obtained with HPCA are typical values expected for the region (approximately 4 keV and 2 cm^{-3}, respectively). MMS first crosses the magnetopause at 13:57 UT (indicated in the plot by the leftmost vertical black line). At this time the magnetic field undergoes a rotation; the z component rotates southward, the y component rotates from slightly dawnward to strongly duskward, and the x component rotates from sunward to antisunward with little change in magnitude. There is also an enhancement in the strength of the magnetic field (Figure 1a), with the magnetosheath magnetic field strength surpassing that of the magnetosphere. Other indicators of the layer transition include a decrease in the proton temperature, from 4 keV to 200 eV, and an increase in proton density, from 2 cm^{-3} to 30 cm^{-3} (Figure 1f). During the period from 14:06 UT to 14:13 UT, MMS-4 encounters the magnetopause

current layer several times. These encounters are indicated by the full and partial rotations of the magnetic field from southward to northward and back, and by the associated changes in temperature and density. By 14:13 UT, the spacecraft exits the magnetosphere and ends up in the magnetosheath.

During the first magnetopause crossing at 13:57 UT, FPI-DES measures a reduction in the omnidirectional electron flux in the energy range from several hundred eV to a few keV (Figure 1b). In the subsequent encounters with the magnetopause boundary layers (14:06–14:13 UT), the electron fluxes intensify once again. This corresponds to a population with higher field-aligned velocities (greater than the mostly isotropic bulk population) in the electron and proton distribution functions (see Figure S1). A similar profile is seen for both the energetic protons and oxygen ions from HPCA (Figures 1c and 1d). In the magnetosphere, the omnidirectional fluxes at energies above a few keV are high for both ion species. In the magnetosheath, the proton flux at high energies is reduced and the high-energy oxygen fluxes nearly vanish. As with the electrons, these high-energy fluxes are observed again when the LLBL and MSBL are encountered later in the interval.

The proton velocity (Figure 1e) from HPCA is generally low in the magnetosphere, less than 100 km/s for each of the individual components. Within the magnetosheath, the magnitude increases to a few hundred kilometers per second. In addition, there are accelerated flows during the initial magnetopause crossing and brief crossings into and out of the magnetosphere from 14:08 UT to 14:11 UT. Interestingly, there does not appear to be a plasma jet associated with the magnetic field rotation from 14:06 to 14:07 UT, although there is a more pronounced enhancement in v_Z between 14:07 and 14:08 UT. This may indicate that MMS4 encountered a "bulge" at the magnetopause as suggested by *Phan et al.* [2004] or that MMS4 passed through a flux transfer event [*Øieroset et al.*, 2016]. It is lastly important to note the orientation of the velocity components within the magnetosheath. The *y* component is directed consistently duskward (positive), while the *x* and *z* components are always directed negatively (indicating antisunward and southward flow, respectively). These velocity profiles are consistent with the spacecraft being located south of the equator on the dusk flank. Further evidence that MMS4 was in a region of ongoing magnetic reconnection is seen in burst mode and fast survey moment calculations using data from the FPI ion instruments on board the spacecraft. The plots in the supporting information show magnetopause crossings from 12:00 to 16:00 on 28 August 2016. At each magnetopause crossing directional jets were encountered; at some there were flow reversals in these jets. It is also important to note that these signatures are absent as expected when the spacecraft is in the magnetosheath or in the magnetosphere. The directional jets, flows, and the associated changes in the magnetic field components are clear indicators of ongoing reconnection.

Figure 2 shows the parallel and antiparallel-streaming 500 eV electrons from EDI (b and c), as well as the directional proton and oxygen ion fluxes from 1 eV to 40 keV (d–g). The changes in the directions of the higher-energy ion fluxes (tens of keV) indicate that the reconnection site moves relative to MMS several times throughout the time interval. In the magnetosphere, the parallel and antiparallel electron fluxes are high and balanced. As MMS-4 crosses the magnetopause (the leftmost orange shaded box), the parallel electron counts drop, while the antiparallel electrons persist for approximately 6–7 s longer. With B_z oriented southward (see Figure 2a), the antiparallel electrons are then propagating northward, indicating that the reconnection site is below the spacecraft at this time.

At 13:59 UT, MMS-4 once again encounters the MSBL (orange shaded region containing the dotted, orange vertical line). The MSBL is distinguished from the magnetosheath by the enhancements of higher-energy H^+ and O^+, as well as enhancements of field-aligned electrons. Because this crossing occurs during southward IMF, the MSBL is differentiated from the LLBL to zeroth order by the direction of B_z (i.e., $-B_z$ for the MSBL and $+B_z$ for the LLBL). During this encounter, a switch in the flow directions from predominantly antiparallel to parallel streaming is seen for both the 500 eV electrons and the higher-energy protons ($>$4 keV) (Figures 2b–2e). The switch in the streaming direction indicates that the reconnection site has moved northward above the spacecraft. MMS-4 more than likely did not traverse the diffusion region during this MSBL encounter because, as the ion moments in Figure 1 suggest, it was not in the current layer as the reversal of streaming directions occurred. Brief bursts of antiparallel electrons and protons between 14:00 and 14:05 UT indicate that the reconnection site moved southward, below the spacecraft during this period (see Figures 2c and 2e).

MMS-4 enters the MSBL at 14:05:20 UT. Particle fluxes seen here are again predominantly antiparallel indicating the reconnection site is still below the spacecraft. When MMS-4 reenters the magnetosphere around 14:08 UT, there is still a predominant antiparallel flux. However, this changes from 14:10 UT to 14:12 UT, where

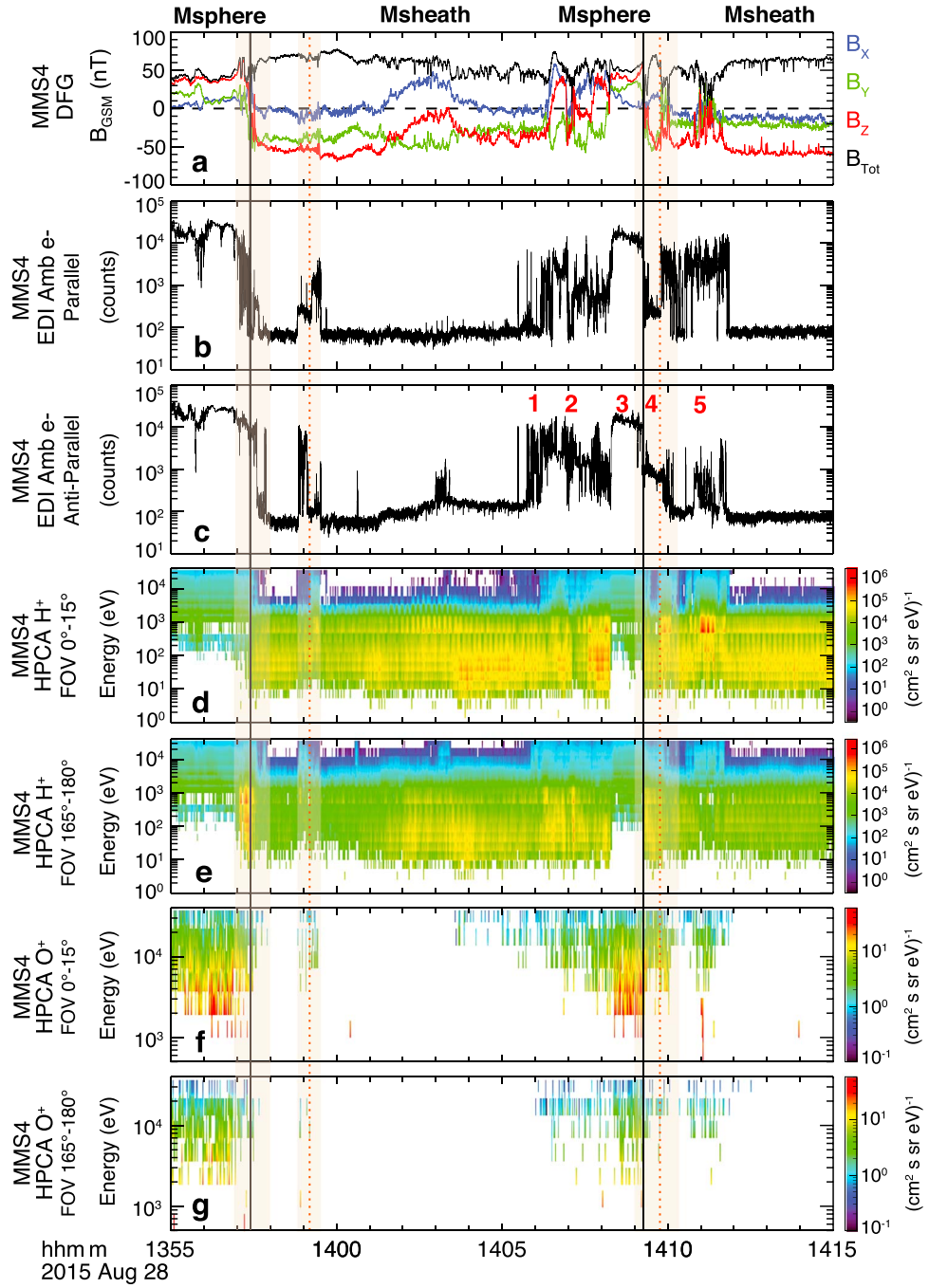

Figure 2. MMS4 magnetic field, directional electron counts, and H^+ and O^+ fluxes during the magnetopause crossing on 28 August 2015. (a) Magnetic field in GSM, as in Figure 1. (b) Ambient electron counts (with energy of ~500 eV) from EDI with pitch angles of 0° (parallel-streaming electrons). (c) Ambient electron counts from EDI with pitch angles of 180° (antiparallel-streaming electrons). (d) Downward flowing H^+ flux from HPCA (the field of view (FOV) of HPCA is with respect to the spacecraft, so a FOV of 0°–15° corresponds to a downward or $-Z$ flow). Because of the southward IMF during the magnetosheath interval, this flow is largely parallel to the magnetic field in the magnetosheath. (e) Upward flowing H^+ flux from HPCA (like in Figure 2c, because of the southward IMF in the magnetosheath, this corresponds to antiparallel flow in the magnetosheath). (f) Downward flowing O^+ flux. (g) Upward flowing O^+ flux. The two black vertical lines are the magnetopause crossings marked in Figure 1. The orange shaded boxes correspond to times shown in Figure 3, marking the initial magnetopause crossing, an encounter with the current layer, and the second crossing back into the magnetosheath. The orange dashed lines mark the switch in flow direction of the ions and electrons observed by EDI and HPCA, signifying the movement of the reconnection site above or below MMS4. The numbers correspond to times along the trajectory of MMS4 marked in Figure 3.

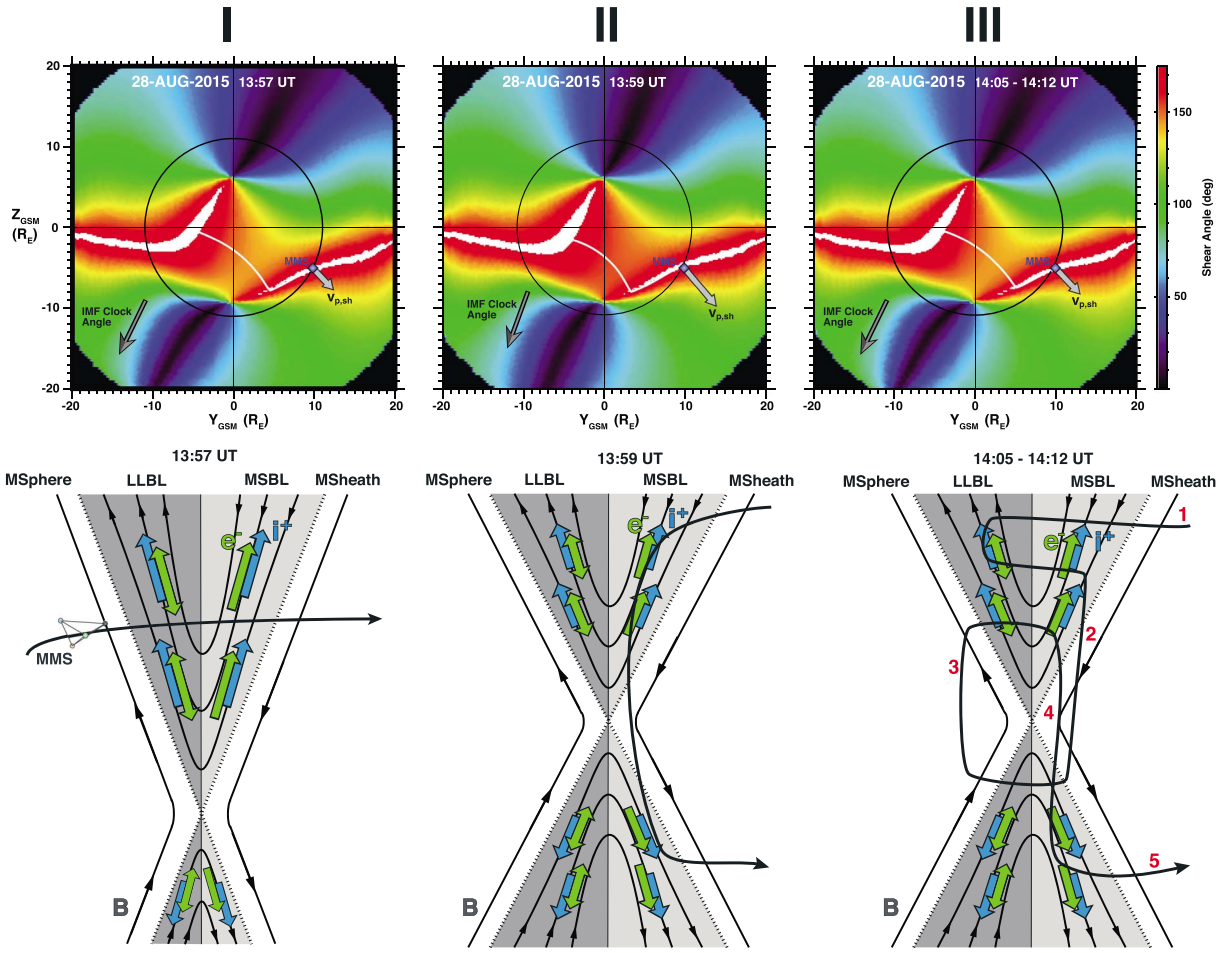

Figure 3. (top) Results of the maximum magnetic shear model for MMS during the encounter with the magnetopause on 28 August 2015. The bulk H^+ velocity in the magnetosheath (light grey arrow, projected into the *Y-Z* GSM plane) observed by MMS (blue diamond) is shown, as is the IMF clock angle (dark grey arrow). (I) Model results for 13:57 UT, with an IMF clock angle of 206°, showing MMS very close to the antiparallel reconnection line on the southern dusk flank. (II) Model results for 13:59 UT, with a clock angle of 200°, where the reconnection line has moved north of (above) MMS. (III) Model results for 14:10 UT (representative of the interval from 14:05 to 14:12 UT), where the clock angle is 206°, and the reconnection line has moved southward from its location at 13:59 UT. (Bottom) Sketches of the MMS trajectory relative to the X line for the times shown for the maximum magnetic shear model. (I) MMS crosses the magnetopause at 13:57:23 UT above the reconnection site. (II) While in the magnetosheath, MMS encounters the current layer from 13:58:50 to 13:59:31 UT, during which the position of the reconnection site moves northward of (above) MMS. (III) After reentering the magnetosphere above the reconnection site, MMS crosses back into the magnetosheath at 14:09:17 UT initially above the reconnection site. Flow directions also reverse at 14:09:47 UT, with MMS leaving the MSBL below the reconnection site by 14:11:52 UT. Magnetosheath flows for these three times have an average $v_{p,x}$ component of −185 km/s.

the measured flux is now largely parallel (rightmost orange shaded region in Figure 2); the reconnection site is now above the spacecraft and remains above MMS-4 while it crosses the boundary layers out to the magnetosheath. Like the observations at 13:59–14:00, MMS does not pass through the diffusion region during the brief encounters with the current layer, since only large southward jets are observed instead of a reversal in the flow direction. During the partial crossings from 14:05:20 UT through 14:12 UT (including the rightmost orange shaded area in Figure 2), EDI parallel and antiparallel counts show possible instances of bidirectional streaming electrons in the MSBL (Figures 2b and 2c). This suggests that MMS-4 may have been between two active reconnection sites [*Hasegawa et al.*, 2010; *Fuselier et al.*, 2011].

Another item to note is that the O^+ fluxes at energies >2 keV show a general agreement with the proton and electron fluxes (see Figure 2). While these trends are echoed, one must exercise caution with the interpretation. Energetic oxygen ions have large gyroradii (tens of kilometers given the ion energy and local magnetic field) and can thus scatter across the magnetopause rather than follow newly opened field lines in the reconnection exhaust [*Wang et al.* 2014]. This "leakage" of energetic O^+ can be seen especially well from approximately 14:04 UT to 14:10 UT (Figures 2f and 2g).

3. Interpretation

An explanation for the events during this time period is shown in Figure 3. The top panel of Figure 3 shows results of the maximum magnetic shear model (projected onto the *Y-Z* GSM plane) for three times corresponding to the orange boxes in Figure 2 (13:57 UT, 13:59 UT, and 14:05 UT–14:12 UT). The colors correspond to the modeled magnetic shear angle, with the white areas in Figure 2a showing the locations where the shear angle is 180° or locally maximized. The IMF clock angle also is shown at the lower left in each panel along with the proton velocity in the magnetosheath ($v_{p,sh}$). The maximum magnetic shear model provides a global context for the interpretation of the MMS4 observations. Although the model has reported uncertainties for distances within 1 R_E [see *Trattner et al.* 2007b], the maximum magnetic shear model has been tested with several missions and simulations and has been shown to be fairly accurate [e.g., *Dunlop et al.*, 2011; *Fuselier et al.*, 2011; *Trattner et al.*, 2012; *Komar et al.*, 2015]. MMS is very close (within 1 R_E) to the predicted antiparallel reconnection line during the magnetopause crossings from 13:55 UT to 14:15 UT. The bottom panels of Figure 3 show the notional motion of the spacecraft through the reconnection region for the three time periods. The spacecraft are virtually stationary with respect to the motion of the reconnection site (i.e., the MMS velocity is ~1 km/s).

In Figure 3(I) the MMS spacecraft are crossing near the reconnection line from the magnetosphere to the magnetosheath, as indicated by the arrow in the lower panel. This crossing occurs north of (above) the reconnection region as indicated by the antiparallel ion and electron fluxes (Figure 2). The crossing is not as simple as shown in Figure 3 (bottom panel) because the magnetopause and boundary layers oscillate back and forth somewhat during the crossing. However, the crossing occurs with the reconnection site below the spacecraft. In the second panel (II), the spacecraft remains on the magnetosheath side of the magnetopause, crossing into the MSBL, but not the magnetopause current layer. As depicted in Figure 3(II) and suggested by the switch in the plasma streaming direction in Figure 2 the reconnection line is initially southward of (below) the spacecraft but then moves above the spacecraft. The location of the reconnection line from the maximum magnetic shear model is also predicted to move northward of MMS from 13:57 UT to 13:59 UT as the IMF becomes slightly more southward (the clock angle changes from 206° to 200° during this time). The third panel of Figure 3(III, bottom) shows the motion of the reconnection site relative to MMS during a 7 min period encompassing a brief reentry into the magnetosphere and partial crossings of the magnetopause. While the spacecraft transitions from the magnetosheath, through the boundary layers, and into the magnetosphere above the reconnection site, the reconnection line moves above MMS as it exits fully into the magnetosheath (see Figure 2c, numbers 1–5). The results from the maximum magnetic shear model during this time period show the IMF clock angle rotating from 201° to 207°, with the reconnection line moving southward to slightly higher latitudes (see supporting information Movie S1). The top panel of Figure 3(III) shows a representative example of this rotation, although MMS is still predicted to be slightly above the reconnection site.

At this higher-latitude antiparallel reconnection site, the magnetosheath bulk flow has a nonnegligible component in the plane of the reconnection site (large tailward $v_{p,x}$ and moderate southward $v_{p,z}$). In boundary normal coordinates (*LMN*, not shown) the flow shear in the *L* direction is approximately 40 km/s, and the predicted X line drift speed (also in the *L* direction) is around −100 km/s [see *Doss et al.*, 2015, equation (5)]. The flow in the *L* direction in the magnetosheath (not shown) is generally sub-Alfvénic ($v_{H,L}/v_{A,L} < 1$, where $v_{A,L}$ is the magnetosheath Alfvén speed). However, during boundary layer encounters in this interval, the flow does exceed the Alfvén speed, particularly from 14:06:15–14:08:00 UT to 14:09:40–14:11:30 UT. From earlier observations and simulations, then, the reconnection site is expected to convect tailward if it is associated with open flux [e.g., *Wilder et al.*, 2014; *Doss et al.*, 2015]. However, the motion of the reconnection site inferred from the MMS-4 observations is generally not associated with the bulk flow of the magnetosheath. Instead, it appears that the motion of the reconnection region is related to minute changes in the IMF clock angle, moving in a relatively north-south direction. This motion is even at times against the magnetosheath bulk flow direction (the reconnection site moves northward toward the equator as the IMF becomes more southward). This suggests the motion of the X line is governed more by the change in IMF direction than the magnetosheath flow.

There remains the possibility that any secondary magnetic islands generated at the reconnection site do convect in the directions of the magnetosheath flow [*Doss et al.,* 2015]. Evidence of bidirectional streaming in the MSBL (see Figures 2a and 2b, around 14:08 UT) suggests the existence of a second active reconnection

site [e.g., *Wilder et al.*, 2014; *Hasegawa et al.*, 2010]. Determining whether these observations are due to relative motion of secondary magnetic islands or to temporally intermittent local reconnection event occurring during this period requires further analysis with observations from all four MMS spacecraft. Another interesting feature of this particular crossing is that while the local magnetic shear is large (see Figure 3), and the magnetic field magnitudes are nearly the same on either side of the magnetopause, MMS4 observes a more special case of the magnetosheath magnetic field being approximately 1.5 times that of the magnetosphere. A more common feature of the Earth's magnetopause, which is observed in this crossing, is a sharp density gradient, with much higher densities in the magnetosheath. The main effects on reconnection and X line motion, then, of these magnetosheath conditions probably arise from the asymmetry in density, and quite a few theoretical and modeling studies have undertaken this particular topic in reconnection [e.g., *Tanaka et al.*, 2008; 2010; *Malakit et al.*, 2010; *Chen et al.*, 2013; *Doss et al.*, 2015]. However, to what extent the effect of the larger magnetic field with the larger densities may have on asymmetric reconnection merits further investigation. It should also be noted that anisotropies are present (as seen from 14:01 to 14:05 UT in Figures 2b and 2c) that are likely due to heating from the bow shock and possibly Hall electrons [e.g., *Tanaka et al.*, 2008]. Whether and to what extent the electron distributions presented here are composed of these Hall electrons requires further in-depth analysis and modeling.

4. Conclusions

Observations of the dusk flank magnetopause by MMS on 28 August 2015 show that antiparallel magnetic reconnection is a stable process even at the dawn-dusk terminator. During this magnetopause encounter, motion of the reconnection site appears not to be a consequence of the magnetosheath bulk ion flow. Instead, the motion is related to small changes in the IMF clock angle, and it cannot be attributed to changes in spacecraft position. The motion is seen to occur as the IMF slightly and slowly rotates, despite increases in the magnetosheath bulk flow speed from sub- to super-Alfvénic flow velocities. These results do not necessarily disagree with the theoretical predictions of convection of the reconnection site due to large flow shears; more work is needed in analyzing observations from all four MMS spacecraft to address the possibility of multiple reconnection sites and secondary magnetic islands during this crossing.

Acknowledgments
The Magnetospheric Multiscale mission required great resources of time and manpower to make collecting these data possible. This work is dedicated to the persons who contributed to this arduous task. Solar wind data from the Wind spacecraft are from the CDAWeb. All data from the first 6 months of the mission are now available to the general public through the MMS Science Data Center at https://lasp.colorado.edu/mms/sdc/public/. The equatorial view of the orbit (in GSE) is available for 28 August 2015 on the public MMS Science Data Center site, as well as through the Van Allen Probes Science Gateway multimission orbit plotter at http://rbspgway.jhuapl.edu/ExtendedMissionOrbit.

References

Burch, J. L., T. E. Moore, R. B. Torbert, and B. L. Giles (2015), Magnetospheric Multiscale overview and science objectives, *Space Sci. Rev.*, doi:10.1007/s11214-015-0164-9.

Cowley, S. W. H., and C. J. Owen (1989), A simple illustrative model of open flux tube motion over the dayside magnetopause, *Planet. Space Sci.*, *37*, 1461–1475, doi:10.1016/0032-0663(89)90116-5.

Chen, Y., C. Xiao, X. Wang, J. Wang, H. Zhang, Z. Pu, Z. Ma, and Z. Guo (2013), The influence of out-of-plane shear flow on Hall magnetic reconnection and FTE generation, *J. Geophys. Res. Space Physics*, *118*, doi:10.1002/jgra.50417.

Doss, C. E., C. M. Komar, P. A. Cassak, F. D. Wilder, S. Eriksson, and J. F. Drake (2015), Asymmetric magnetic reconnection with a flow shear and applications to the magnetopause, *J. Geophys. Res. Space Physics*, *120*, 7748–7763, doi:10.1002/2015JA021489.

Dunlop, M. W., et al. (2011), Magnetopause reconnection across wide local time, *Ann. Geophys.*, *29*, 1683–1697, doi:10.5194/angeo-29-1683-2011.

Frey, H. U., T. D. Phan, S. A. Fuselier, and S. B. Mende (2003), Continuous magnetic reconnection at Earth's magnetopause, *Nature*, *426*, 533–537, doi:10.1038/nature02084.

Fuselier, S. A., B. J. Anderson, and T. G. Onsager (1997), Electron and ion signatures of field line topology at the low-shear magnetopause, *J. Geophys. Res.*, *102*, 4847–4863, doi:10.1029/96JA03635.

Fuselier, S. A., S. M. Petrinec, and K. J. Trattner (2000), Stability of the high-latitude reconnection site for steady northward IMF, *Geophys. Res. Lett.*, *27*, 473–476, doi:10.1029/1999GL003706.

Fuselier, S. A., S. M. Petrinec, and K. J. Trattner (2011), Antiparallel and component reconnection at the dayside magnetopause, *J. Geophys. Res.*, *116* A10227, doi:10.1029/2011JA016888.

Gosling, J. T., M. F. Thomsen, S. J. Bame, and C. T. Russell (1986), Accelerated plasma flows at the near-tail magnetopause, *J. Geophys. Res.*, *91*(A3), 3029–3041, doi:10.1029/JA091iA03p03029.

Gosling, J. T., M. F. Thomsen, S. J. Bame, T. G. Onsager, and C. T. Russell (1990), The electron edge of the low latitude boundary layer during accelerated flow events, *Geophys. Res Letters*, *17*, 1833–1836.

Hasegawa, H., et al. (2010), Evidence for a flux transfer event generated by multiple X-line reconnection at the magnetopause, *Geophys. Res Letters*, *37*, L16101, doi:10.1029/2010GL044219.

Hasegawa, H., et al. (2016), Decay of mesoscale flux transfer events during quasi-continuous spatially extended reconnection at the magnetopause, *Geophys. Res. Lett.*, *43*, 4755–4762, doi:10.1002/2016GL069225.

Komar, C. M., R. L. Fermo, and P. A. Cassak (2015), Comparative analysis of dayside magnetic reconnection models in global magnetosphere simulations, *J. Geophys. Res. Space Physics*, *120*, 276–294, doi:10.1002/2014JA020587.

Malakit, K., M. A. Shay, P. A. Cassak, and C. Bard (2010), Scaling of asymmetric magnetic reconnection: Kinetic particle-in-cell simulations, *J. Geophys. Res.*, *115*, doi:10.1029/2010JA015452.

Moore, T. E., M.-C. Fok, and M. O. Chandler (2002), The dayside reconnection X line, *J. Geophys. Res.*, *107*(A10), 1332, doi:10.1029/2002JA009381.

Øieroset, M., et al. (2016), MMS observations of large guide field symmetric reconnection between colliding reconnection jets at the center of a magnetic flux rope at the magnetopause, *Geophys. Res. Lett.*, *43*, doi:10.1002/2016GL069166.
Petrinec, S. M., K. J. Trattner, and S. A. Fuselier (2003), Steady reconnection during intervals of northward IMF: Implications for magnetosheath properties, *J. Geophys. Res.*, *108*(A12), 1458, doi:10.1029/2003JA009979.
Phan, T.-D., et al. (2000), Extended magnetic reconnection at the Earth's magnetopause from detection of bi-directional jets, *Nature*, *404*, 848–850.
Phan, T.-D., et al. (2004), Cluster observations of continuous reconnection at the magnetopause under steady interplanetary magnetic field conditions, *Ann. Geophys.*, *22*, doi:10.5194/angeo-22-2355-2004.
Phan, T.-D., et al. (2006), A magnetic reconnection X-line extending more than 390 Earth radii in the solar wind, *Nature*, *439*, 175–177.
Pollock, C., et al. (2016), The Fast Plasma Investigation for Magnetospheric Multiscale, *Space Sci. Rev.*, *199*, doi:10.1007/s11214-016-0245-4.
Russell, C. T., et al. (2014), The Magnetospheric Multiscale magnetometers, *Space Sci. Rev.*, doi:10.1007/s11214-014-0057-3.
Tanaka, K. G., et al. (2008), Effects on magnetic reconnection of a density asymmetry across the current sheet, *Ann. Geophys.*, *26*, 2471–2483, doi:10.5194/angeo-26-2471-2008.
Tanaka, K. G., M. Fujimoto, and I. Shinohara (2010), Physics of magnetopause reconnection: A study of the combined effects of density asymmetry, velocity shear, and guide field, *Int. J. Geopyhs.*, *2010*, doi:10.1155/2010/202583.
Torbert, R. B., et al. (2016), The Electron Drift Instrument for MMS, *Space Sci. Rev.*, *199*, doi:10.1007/s11214-015-0182-7.
Trattner, K. J., J. Mulcock, S. M. Petrinec, and S. A. Fuselier (2007a), The location of the reconnection line at the magnetopause during southward IMF conditions, *Geophys. Res. Letters*, *34* L03108, doi:10.1029/2006GL028397.
Trattner, K. J., J. S. Mulcock, S. M. Petrinec, and S. A. Fuselier (2007b), Probing the boundary between antiparallel and component reconnection during southward interplanetary magnetic field conditions, *J. Geophys. Res.*, *112*, A08210, doi:10.1029/2007JA012270.
Trattner, K. J., S. M. Petrinec, S. A. Fuselier, and T. D. Phan (2012), The location of reconnection at the magnetopause: Testing the maximum magnetic shear model with THEMIS observations, *J. Geophys. Res.*, *117*, A01201, doi:10.1029/2011JA016959.
Trenchi, L., M. F. Marcucci, G. Pallocchia, G. Consolini, M. B. Bacassano Cattaneo, A. M. Di Lellis, H. Reme, L. Kistler, C. M. Carr, and J. B. Cao (2008), Occurrence of reconnection jets at the dayside magnetopause: Double star observations, *J. Geophys. Res.*, *113*(A07S10), 1458, doi:10.1029/2007JA012774.
Vines, S. K., S. A. Fuselier, K. J. Trattner, S. M. Petrinec, and J. F. Drake (2015), Ion acceleration dependence on magnetic shear angle in dayside magnetopause reconnection, *J. Geophys. Res. Space Physics*, *120*, doi:10.1002/2015JA021464.
Wang, R., R. Nakamura, T. Zhang, A. Du, W. Baumjohann, Q. Lu, and R. Z. Fazakerley (2014), Evidence of transient reconnection in the outflow jet of primary reconnection site, *Ann. Geophys.*, *32*, 239–248, doi:10.5194/angeo-32-239-2014.
Wilder, F. D., S. Eriksson, K. J. Trattner, P. A. Cassak, S. A. Fuselier, and B. Lybekk (2014), Observation of a retreating x line and magnetic islands poleward of the cusp during northward interplanetary magnetic field conditions, *J. Geophys. Res. Space Physics*, *119*, 9643–9657, doi:10.1002/2014JA020453.
Young, D. T., et al. (2014), Hot Plasma Composition Analyzer for the Magnetospheric Multiscale mission, *Space Sci. Rev.*, doi:10.1007/s11214-014-0049-6.